



OPEN

## Biogenic synthesis of silver nanoparticles using *Zaleya pentandra* and investigation of their biological activities

Neelam Neelam<sup>1</sup>, Faizan Ullah<sup>1✉</sup>, Modhi O. Alotaibi<sup>2,3</sup>, Nashad Ali<sup>1</sup>, Tahir Iqbal<sup>1</sup>, Sultan Mehmood<sup>1</sup>, Muhammad Mudasar Aslam<sup>1</sup>, Umar Nawaz Khan<sup>4</sup>, Adel M. Ghoneim<sup>5</sup>, Esawy Mahmoud<sup>6</sup>, Taufiq Nawaz<sup>7</sup>, Shah Saud<sup>8</sup> & Shah Fahad<sup>9✉</sup>

This study reports a sustainable and eco-friendly approach for the green synthesis and optimization of silver nanoparticles (AgNPs) utilizing the *Zaleya pentandra* stem extract (ZSE). Critical reaction parameters including temperature (25 °C), pH (9.0), extract volume (200 µL), and incubation duration (24 h) were systematically optimized to enhance green-synthesized AgNPs yield. Successful synthesis of AgNPs was confirmed by UV-Vis spectroscopy, exhibiting a distinct surface plasmon resonance (SPR) peak at 426 nm. The FT-IR spectroscopy revealed phytochemical functional groups acting as bioreductants and capping agents. Morphological and structural characterizations using Field Emission Scanning Electron Microscope (FESEM) and XRD confirmed the formation of predominantly spherical nanoparticles, while EDX spectroscopy validated silver as pure element with minor contributions from plant-derived elements likely associated with phytochemical capping or sample preparation. The green-synthesized AgNPs displayed potent antibacterial efficacy, with inhibition zones of 30.9 mm (*Staphylococcus aureus*), 27.6 mm (*Klebsiella pneumoniae*), and 25.0 mm (*Escherichia coli*). In antifungal assays, the green-synthesized AgNPs achieved > 97% mycelial growth inhibition against a spectrum of phytopathogenic fungi. Antioxidant potential assessed via DPPH radical scavenging assay yielded a significant  $IC_{50}$  value of 199.07 µg/mL for the green-synthesized AgNPs. Notably, the green-synthesized AgNPs exhibited strong  $\alpha$ -glucosidase inhibitory activity ( $IC_{50}$ : 67.059 µg/mL), surpassing the efficacy of the standard drug acarbose ( $IC_{50}$ : 77.42 µg/mL). These multifunctional silver nanoparticles, synthesized via an optimized process and a green route using *Z. pentandra* stem extract demonstrated significant promise for applications in antimicrobial, antioxidant, and antidiabetic therapeutics, underscoring their potential role in next-generation nanomedicine.

**Keywords** *Zaleya pentandra*, Green nanotechnology, Silver nanoparticles, Antimicrobial properties, Antioxidant capacity,  $\alpha$ -glucosidase inhibition

Recently, nanotechnology has developed as an emerging field of research due to its extensive applications in medicine, agriculture, and the food industry<sup>1</sup>. Nanoparticles, with sizes ranging from 1 to 100 nm, possess a large surface area to volume ratio and unique chemical properties, which contribute to their antimicrobial capabilities<sup>2</sup>. Metal-based nanoparticles are highly popular due to their diverse industrial applications<sup>3</sup>.

Metallic nanoparticles are synthesized through physical and chemical methods which requires expensive equipment and results in the generation of toxic wastes. Therefore, recently green synthesis of metallic nanoparticles by using biological materials has gained popularity<sup>4</sup>. This approach includes utilizing capping

<sup>1</sup>Department of Botany, University of Science and Technology Bannu, Bannu, Pakistan. <sup>2</sup>Department of Biology, College of Science, Princess Nourah bint Abdulrahman University, P.O. Box 84428, Riyadh 11671, Saudi Arabia.

<sup>3</sup>Environmental and Biomaterial Unit, Natural and Health Sciences Research Center, Princess Nourah bint Abdulrahman University, P.O. Box 84428, Riyadh 11671, Saudi Arabia. <sup>4</sup>Nanosciences and Technology Department, National Centre for Physics, Islamabad, Pakistan. <sup>5</sup>Agricultural Research Center, Field Crops Research Institute, Giza 12112, Egypt. <sup>6</sup>Soil and Water Department, Faculty of Agriculture, Tanta University, Tanta, Egypt. <sup>7</sup>Department of Biology and Microbiology, South Dakota State University, Brookings, SD 57007, USA. <sup>8</sup>College of Life Science, Linyi University, Linyi 276000, Shandong, China. <sup>9</sup>Department of Agronomy, Abdul Wali Khan University Mardan, Mardan 23200, Khyber Pakhtunkhwa, Pakistan. ✉email: drfaizanwazir@gmail.com; shah\_fahad80@yahoo.com

and reducing properties of biological materials instance plant extracts, fungi, bacteria, and others<sup>5,6</sup>. Green synthesis is a straightforward, less time consuming, eco-friendly, and cost effective method of nanoparticles synthesis<sup>7</sup>. This green synthesis approach not only reduces the use and production of harmful chemicals but also aids the synthesis of metallic nanoparticles in mild conditions. However, during the biosynthesis process reaction variables such as temperature, pH of media, incubation time, and concentration of the biological extract significantly effects the yield, size and properties of the nanoparticles. The phytosynthesis of nanoparticles is also influenced by the type of plant species, its geographical and seasonal distributions and types of biomolecules. Therefore, it is necessary to carefully select the biological material and monitor the reaction conditions impacting the size, shape, and surface of the nanoparticles<sup>8,9</sup>. Although the mechanism of nanoparticle synthesis by using plant extracts is not well known, it is believed that various biomolecules found in plant extracts, such as terpenoids, enzymes, carbohydrates, alkaloids, phenols, flavonoids, and proteins, play a major role in the reduction of metal ions during the phytosynthesis of nanoparticles<sup>10-12</sup>.

Biologically produced silver nanoparticles (AgNPs) represent considerable interest with an eco-friendly and sustainable alternative to the traditional chemical methods. Silver salt solutions ( $\text{AgNO}_3$ ) are utilized as the precursor solutions for the production of AgNPs. Biological extract is introduced with the precursor solutions, and the reducing agents of biological material mediate silver ions reduction to produce silver nanoparticles<sup>13</sup>. The novel application of silver nanoparticles includes its combination with material science to address global challenges<sup>14</sup>. Recently, it has been investigated that silver nanoparticles are highly antimicrobial compared to other commercially available metal oxide nanoparticles<sup>15</sup>. Silver nanoparticles possess antimicrobial, antiviral, anti-cancer and anti-diabetic activities<sup>5,8</sup>. Asif et al.<sup>16</sup> synthesized silver nanoparticles by using leaf extract of *Moringa oleifera*. The resulting nanoparticles were spherical in shape with particle size 10 nm to 25 nm showing strong antibacterial activities. Bhati et al.<sup>17</sup> synthesized silver nanoparticles using *Artemisia scoparia* extract and reported their effectiveness as antibacterial agent.

*Zaleya pentandra* L. (African purslane) is an annual weed that thrives well in dry and semiarid environments and belongs to the family Aizoaceae. It is mainly distributed in Africa, Iran, Pakistan, and India<sup>18</sup>. Traditionally, *Z. pentandra* treats malaria and snake bites<sup>19</sup>. It has digestive and stomachic properties and can treat respiratory tract infections and coughs<sup>20</sup>. The anti-diabetic properties of *Z. pentandra* has been reported<sup>21</sup>. The *Z. pentandra* possesses phytochemicals like alkaloids, phenolics, terpenoids, fatty acid derivatives, and carbohydrates with potent antioxidant properties<sup>22</sup>. African purslane has been reported as a highly consumed plant for traditional medicine. *Zaleya pentandra* plays a significant role due to its capability to overcome challenging conditions and explore the potential cultivations in different areas, providing a convenient option for food security<sup>23</sup>. The above mentioned medicinal properties and phytochemical composition signifies the biomedical applications of the *Z. pentandra*.

Due to its strong phytochemical profile, this study has used *Z. pentandra* stem aqueous (water) extract for the green-synthesis of AgNPs. However; the AgNPs green-synthesis requires optimized conditions such as biological extract concentration, pH of the aqueous phase, synthesis temperature, incubation time, and silver salt concentration<sup>24,25</sup>. Presently no optimized protocol is available for the green-synthesis of AgNPs using stem aqueous (water) extract of *Z. pentandra*. Moreover, this study has used water as a solvent for plant's extract preparation as it is ecologically more safe, highly compatible with biological systems and effective in the extraction of certain phytochemicals like phenolics and flavonoids which play significant role in the green-synthesis of nanoparticles. The current research developed an optimized protocol for the synthesis of AgNPs using an aqueous (water) stem extract of *Z. pentandra* (ZSE). After characterization of the ZSE synthesized AgNPs using advanced analytical techniques, they were tested for in vitro antimicrobial, antioxidant, and antidiabetic activities.

## Materials and methods

### Formation of *Z. pentandra* extract

Fresh plants of *Z. pentandra* Fig. 1 were collected from District Bannu (32.9298 °N and 70.6693 °E) Pakistan. This plant species is frequently found in the collection region and has been reported neither threatened nor endangered. After authenticating taxonomically, the specimen was issued a voucher number Zp-2023-03 and deposited in the herbarium of the Botany Department University of Science & Technology Bannu Pakistan. The plants were rinsed three times with tap water and shade-dried for one week to get rid of the dust. After defoliating, the dried stems of 100 plants were finely crushed and sieved using a sieve plate (5 mm particle size). The 20 g stem powder was extracted in 1000 mL distilled water for three days with continuous shaking and then filtered using a Whatman grade 1 filter paper. The extract obtained was called 2% *Z. pentandra* stem extract (ZSE).

### Preparation of silver nitrate solution

The 50 mL of  $\text{AgNO}_3$  solution (0.01mM) was diluted with distilled water to obtain 100 mL 0.001 mM  $\text{AgNO}_3$  solution. The solution was transparent and free of any kind of solid particles.

### The ZSE-mediated synthesis of silver nanoparticles

For the synthesis of AgNPs, a 5 mL solution of  $\text{AgNO}_3$  (0.001 mM) was mixed with different concentrations (100, 200, 300  $\mu\text{L}$ ) of ZSE (2%). The resultant mixtures were constantly stirred at various temperature ranges (5 °C to 45 °C) for 24 h. The pH of the solutions (initial pH of the extract being 5.6) was maintained from 2 to 9 by drop wise addition of 0.1 M HCl or 0.1 mM NaOH solution. The solid AgNPs were separated by centrifugation the mixture at 8000 x g for ten minutes. The centrifugation procedure was repeated twice to remove free silver ions and obtain the maximum amount of AgNPs as a solid pellet. The final black pellet was dried in an oven for



**Fig. 1.** *Zaleya pentandra*.

24 h at 60 °C and ground finely. The powder was stored in a closed container for characterization and biological activities.

#### Characterization of green-synthesized silver nanoparticles

The AgNPs green-synthesis was confirmed by recording the UV-Vis absorption spectra of samples at wavelength 190 to 800 nm. The absorbance spectra were recorded using Shimadzu (Japan) UV/visible scanning spectrophotometer. The ZSE and the resulting nanoparticles were evaluated for the occurrence of various biomolecules using Fourier Transform Infrared spectroscopy (Nicolet 6700 FT-IR instrument). The ZSE and the resulting nanoparticles were evaluated at room temperature for the occurrence of various biomolecules using Fourier Transform Infrared spectroscopy (Nicolet 6700 FT-IR instrument) using KBr method. The spectrum measurements were confirmed in the range of 400-4,000  $\text{cm}^{-1}$ . The Field Emission Scanning Electron Microscope (Model sigma 500 VP) attached with an Energy Dispersive X-Ray (Oxford instrument) determined the morphology of the green-synthesized AgNPs and the prevalence of Ag element. The green-synthesized AgNPs 1 mg was used for making a thin film on a carbon tape and then coated it with platinum. Multiple microscopic images were prepared using different magnification images. The crystal structure of the green-synthesized AgNPs was determined by X-ray crystallography technique (Bruker-D8 XRD machine). The machine was operated at 30 mA/40 kV with Cu K $\alpha$  radiation in the 2 $\theta$  range of 20–80 for analyzing crystallinity of the green-synthesized AgNPs.

#### Biological evaluation of the synthesized AgNPs

##### Antibacterial activity

The green-synthesized AgNPs were tested for antibacterial activity using a method of<sup>26</sup>. Three bacteria, including *Escherichia coli* (ATCC 25922), *Klebsiella pneumoniae* (MTCC 618), and *Staphylococcus aureus* (ATCC 6538), were used in this research study. Freshly prepared cultures of the selected bacteria were streaked on the nutrient agar plates using sterilized 3 cm long cotton swabs. Wells of size 6 mm were prepared in the agar plates by applying a sterilized steel borer. Three suspensions of the AgNPs viz. 1000, 500, and 100  $\mu\text{g}/\text{mL}$  were made in sterilized distilled water by ultra-sonication. Similarly, aqueous (water) solutions of  $\text{AgNO}_3$  (0.001 mM) and *Z. pentandra* extract (2%) were also prepared. The aqueous (water) solution of antibiotic levofloxacin (1 mg/mL) was poured into wells as a positive control, and distilled water (sterilized) was poured into specified wells as a negative control. The wells were fill up with 100  $\mu\text{L}$  suspensions of silver nanoparticles (AgNPs),  $\text{AgNO}_3$  solution, *Z. pentandra* extract, levofloxacin solution, or sterilized distilled water separately. After incubating the Petri plates at 37 °C for 24 h, the zone of bacterial growth inhibition around each well was measured in millimeters.

The green-synthesized AgNPs minimum inhibitory concentration (MIC) effective in growth inhibition of bacteria was determined using the broth dilution method<sup>12</sup>. Different quantities of AgNPs (100, 80, 60, 40, 20, 10, 5, and 2.5  $\mu\text{g/mL}$ ) in deionized water were transferred to sterilized glass test tubes containing 5mL Mueller Hinton broth. Then, 100  $\mu\text{L}$  of fresh bacterial culture adjusted to a 0.5 McFarland suspension was transferred to the test tubes, except for the negative control. The test tubes were incubated for 20 h by setting the incubator thermostat at 37 °C. After completion of the incubation time, the test tubes were evaluated for turbidity by visual comparison with positive and negative controls to confirm the MIC.

#### Antifungal evaluation

The green-synthesized AgNPs and stem extract of *Z.pantandra* were tested for antifungal activity against four fungal species viz. *Fusarium solanii*, *Aspergillus niger*, *Rhizoctonia solani* and *Colletotrichum* sp<sup>27</sup> in a modified way. Sabraud dextrose agar medium 8.16 g/120 mL D.H<sub>2</sub>O was autoclaved for 21 min at 121 °C. 5 mL of this melted media was put into glass test tubes. The test tubes were inverted slanting, and 8 cm long slants were prepared. When the media was cooled to 40 °C then 100  $\mu\text{L}$  of the AgNO<sub>3</sub> (0.001 mM), *Z. pentandra* aqueous extract (100 mg/100mL), *Z. pentandra* aqueous extract 50 mg/100mL, suspensions of green-synthesized AgNPs 100 and 50 mg/100mL were added to the test tubes separately. Each fungal strain's 5 mm diameter mycelial block was kept at the end of each slant. Antifungal terbinafine 3 mg/mL in deionized water and pure deionized controls were considered positive and negative controls. At last, tubes were placed in an incubator for a week at 28 °C.

$$\text{Inhibition in linear growth \%} = 100 - \frac{\text{Linear growth of fungi in control (mm)} - \text{Linear growth of fungi in treatment (mm)}}{\text{Linear growth of fungi in control (mm)}} \times 100$$

#### Antioxidant activity

The capability of green-synthesized AgNPs and *Z. pentandra* stem extract to scavenge free radicals was assessed<sup>28</sup>. Three concentrations of ZSE and green-synthesized AgNPs were prepared in 50% aqueous methanol, i.e. 100, 200 and 300  $\mu\text{g/mL}$ . The reaction was started by mixing 100  $\mu\text{L}$  of AgNPs suspensions or ZSE with 3 mL 1mM DPPH (2, 2-diphenylpicrylhydrazyl) solution. Ascorbic acid solutions of the same concentrations, mentioned above (100, 200, and 300  $\mu\text{g/mL}$ ) were utilized for making control samples. The samples absorbance was measured at 517 nm using a UV/visible spectrophotometer (Perkin-Elmer Lambda 950, UK).

$$\text{DPPH free radical scavenging \%} = \frac{(\text{O.D of control} - \text{O.D of sample})}{(\text{O.D of control})} \times 100$$

#### Antidiabetic activity

The antidiabetic effects of the green-synthesized AgNPs were determined by assessing their inhibitory action on the  $\alpha$ -glucosidase enzyme. The AgNPs suspensions or solutions of standard drug acarbose (10 to 100  $\mu\text{g/mL}$ ) were added to 20% w/v sucrose solution, maintaining the pH at 8.0 in the presence of Tris buffer (0.2 M). The mixtures were incubated at 37 °C for five minutes. Later on, all the samples were added with 1 U/mL  $\alpha$ -glucosidase enzyme. After incubating all the samples at 35 °C for 40 min, 2 mL of the 6 N HCl solution was added to them. All the samples were evaluated for optical density measurements at 540 nm<sup>29</sup>. The  $\alpha$ -glucosidase % inhibition was measured using the formula.

$$\alpha \text{ glucosidase \% inhibition} = \left[ \frac{(\text{absobance value of control} - \text{absorbance value of sample})}{(\text{absorbance value of control})} \right] * 100$$

#### Data analysis

The antimicrobial, antioxidant, and antidiabetic activity data were evaluated using variance analysis and least significant difference tests. The statistical package STATISTIX-10 was used for data analysis. Standard error values were determined using Microsoft excel-10. Linear regression analysis was used to calculate the IC50 values of antioxidant and antidiabetic activity (MLA-“Quest Graph IC50 calculator”). AAT Bioquest, Inc.

### Results and discussion

#### Method optimization for the green-synthesis of AgNPs

The method uses aqueous (water) stem extract of *Z. pentandra* (ZSE 2%) and AgNO<sub>3</sub> solution (0.001mM) for the phyto-synthesis of AgNPs. Different quantities (100, 200, and 300  $\mu\text{L}$ ) of ZSE were mixed with 5 mL AgNO<sub>3</sub> (0.001mM) solution, maintaining pH 2 to 9. The variables like incubation time, temperature, pH, and concentration of ZSE affecting green synthesis of AgNPs were studied in detail. Upon treatment with ZSE, the color of AgNO<sub>3</sub> solution changed to dark brown Fig. 2. The color change of the AgNO<sub>3</sub> solution to brown confirms the existence of silver nanoparticles<sup>30</sup>. Aqueous solutions' color changes mainly due to the surface plasmon resonance phenomenon<sup>31,32</sup>.

#### Incubation time

The working solutions of AgNO<sub>3</sub> added with ZSE were incubated for 12 and 24 h while keeping other reaction conditions at optimum Fig. 3A. After 24 h of incubation, the color of mixture turned dark brown. The UV/Visible spectrophotometry analysis showed a cute peak at 426 nm which is characteristic peak of silver nanoparticles. The appearance of sharp peak at 426 nm after 24 h of incubation means high plasmon band formation due to the conversion of the large amount of Ag<sup>+</sup> into Ag<sup>0</sup><sup>33</sup>. The strong absorption at 426 nm reflects the degradation of silver ions (Ag<sup>+</sup>) by the ZSE and the production of AgNPs. The appearance of the absorption peak at 426 nm



**Fig. 2.** Visual analysis of the change in color of the  $\text{AgNO}_3$  solution to brown that confirms the green-synthesis of AgNPs. Key: ZSE: *Z. pentandra* stem extract.

indicated the production of small-size AgNPs. A broad peak suggests the production of large-size nanoparticles, whereas a sharp peak at lower wavelengths indicates the production of small-size nanoparticles<sup>30</sup>.

#### Temperature

Temperature is a significant variable affecting nanoparticles' synthesis, shape, and size<sup>34</sup>. The AgNPs green-synthesis was influenced by alteration in temperature (5, 15, 25, 25, 45 °C) of the aqueous phase Fig. 3B. The AgNPs creation was verified by measuring the maximum absorption value at 426 nm at 25 °C. A dominant peak at 426 nm confirms the presence and dominancy of AgNPs. With an increase (> 25 °C) or a decrease (< 25 °C) in temperature, the absorbance value was decreased. Low temperature favors better nano-sizing due to the clumping of silver nanoparticles<sup>35</sup>.

#### pH

The AgNP green-synthesis was significantly affected by the most critical parameter, i.e., the  $\text{pH}$  of the media Fig. 3C. The reaction mixtures were prepared at different  $\text{pH}$  (2 to 9). The  $\text{pH}$  9, with 24 h of incubation with all optimum reaction conditions, resulted in maximum absorbance value of 426 nm. A decrease in pH below 7 resulted a significant reduction in absorbance value. This showed that acidic media (pH 2–5) did not favor the AgNPs synthesis suggesting that lower pH inhibited nucleation to form new AgNPs. High pH favors the biosynthesis of Ag nanoparticles<sup>36</sup>. Sharp and narrow bands appear in basic pH due to the ionization process of phenolic compounds occurring in the plant extracts. High pH favors the availability of various functional groups in the plant extracts for silver binding, producing nanoparticles with small diameters<sup>37</sup>. Therefore,  $\text{pH}$  9 is recommended as an ideal pH for the ZSE-mediated AgNPs green-synthesis.

#### Concentration of ZSE

Absorption spectra Fig. 3D of the aqueous phase were recorded at varying concentrations of ZSE (100, 200, and 300  $\mu\text{L}$ ). Maximum absorbance value was recorded by reacting 200  $\mu\text{L}$  ZSE with a 5 mL solution of  $\text{AgNO}_3$  (0.001 mM). This study indicated that green-synthesis of AgNPs was greatly dependent on the concentration of ZSE. Sher et al.<sup>38</sup> also reported similar results during the biosynthesis of AgNPs using plant extract. The plant extract concentration significantly affect the yield, size and shape of the resulting nanoparticles<sup>39</sup>.

#### Characterization of the ZSE synthesized AgNPs

This study used a variety of analytical techniques for the characterization of ZSE green-synthesized AgNPs.

#### Fourier infrared spectroscopy

Fourier infrared spectroscopy (FT-IR) was used to identify different types of biomolecules in *Z. pentandra* stem extract, which reduced silver ions into silver nanoparticles Fig. 4. The *Z. pentandra* stem extract showed several characteristic peaks representing the presence of different kinds of biomolecules in it. The bands appeared at 3344.48, 1625.97, 1374.18, 1317.54, 870.46, and 692  $\text{cm}^{-1}$  were designated to stretching vibration of -OH bond of alcohol, C = C bond of conjugated alkenes, O-H bond of phenolic compounds, C-N bond of aromatic compounds, C-H bending and C-Br bonding of aliphatic bromine compound. A shift of peaks in the phyo-

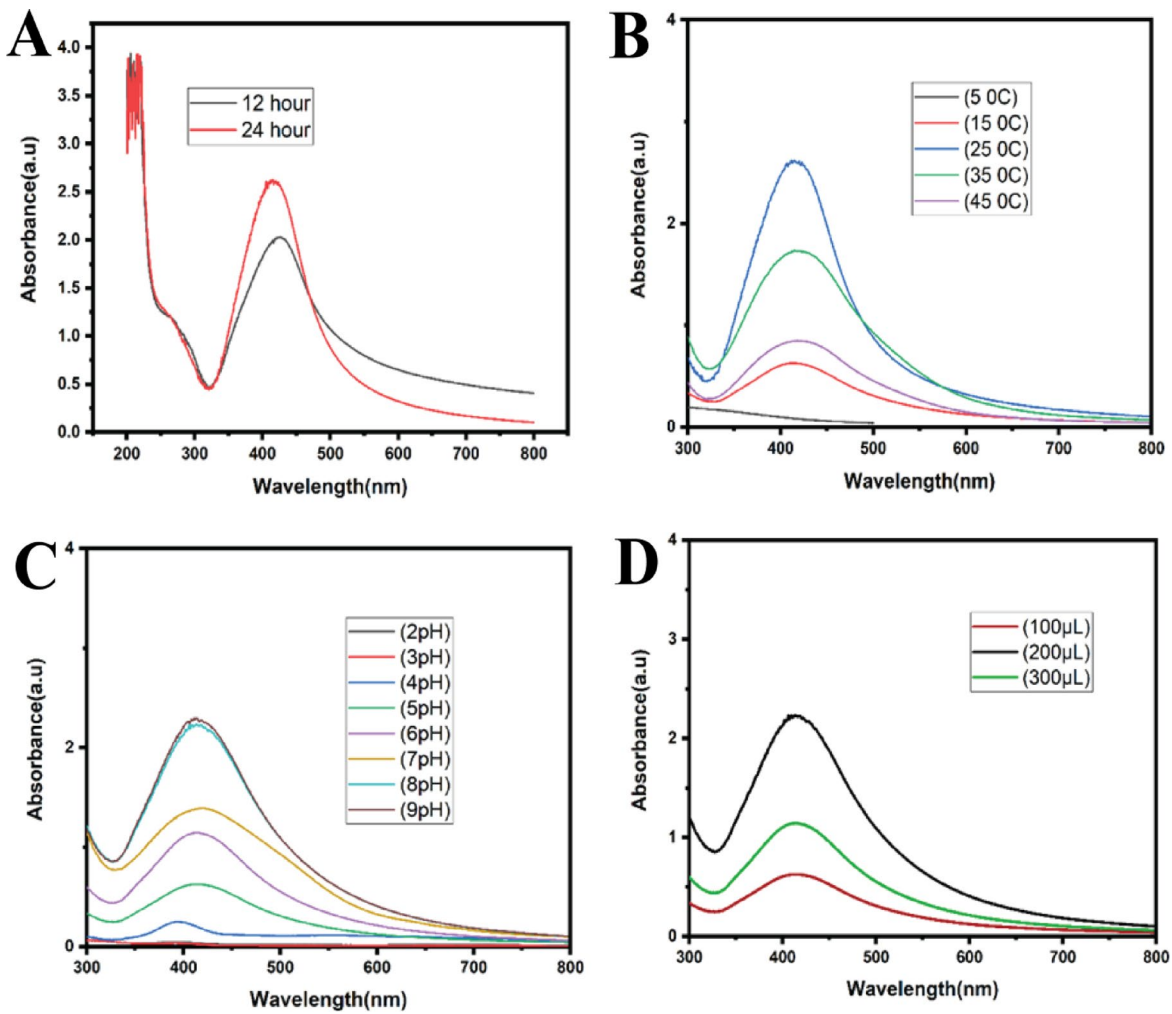


**Fig. 3.** The effect of reaction variables (A) incubation time (B) temperature (C) media pH (D) plant extract concentration on the green-synthesis of AgNPs using *Z. pentandra* stem extract.

synthesized AgNPs suggested that various functional groups found in the *Z. pentandra* stem extract participated in the AgNP formation. In the case of AgNPs, the frequencies for the -OH bond of alcohol, -OH bond of phenolic group and C = C stretching alkene are assigned at 3328.95, 1634.17 and 812.30  $\text{cm}^{-1}$ , while several absorption peaks have disappeared<sup>40</sup>.

#### The XRD analyses

The XRD crystallography ensured the crystalline nature of the green-synthesized AgNPs Fig. 5. The XRD analysis showed four distinct peaks at  $2\theta$ , i.e., 38.2, 44.76, 64.39, and 77.48°, which showed planes of (111), (200), (220), and (311), indicating the crystalline cubic structure of the AgNPs<sup>41</sup>. The peaks of the planes at (111), (200), (220), and (311) were also reported in green synthesized AgNPs using leaf extract of *Cucumis prophetarum*<sup>42</sup>. The peak sharpening provided evidence of the presence of nanoscale particles<sup>43</sup>.

The green-synthesized AgNPs diameter was calculated using the Debye Scherrer formula.

$$D = 0.9 \times \lambda / \beta \cos \theta$$

Where  $\lambda$  = x-ray wavelength,  $B$  = width of FWHM (Full Breath Half Maximum),  $\theta$  = Bragg's angles. According to Debye Scherrer formula the average crystalline size of the green-synthesized AgNPs was 7.78 nm. The average crystalline diameter was smaller than findings of Firdous et al.<sup>44</sup> who reported crystal diameter of 21.80 nm for *Carissa spinarum* derived AgNPs. Ahmad et al.<sup>45</sup> reported that mean crystalline diameter of *Piper cubeba* derived AgNPs was 7–51 nm. These findings suggested that bioactive compounds found in the ZSE were not only responsible for the stabilization but also played important role in providing the crystalline structure of green-synthesized AgNPs<sup>42</sup>.

#### The FESEM analysis

The FESEM analysis revealed that the ZSE synthesized AgNPs were spherical in shape. The FESEM images showed that the average particle size was around 13.68 nm while calculating size of 50 particles using image J software Fig. 6A,B. These findings are consistent with studies of Azizi et al.<sup>46</sup> reporting 12.31 to 35.61 nm particle

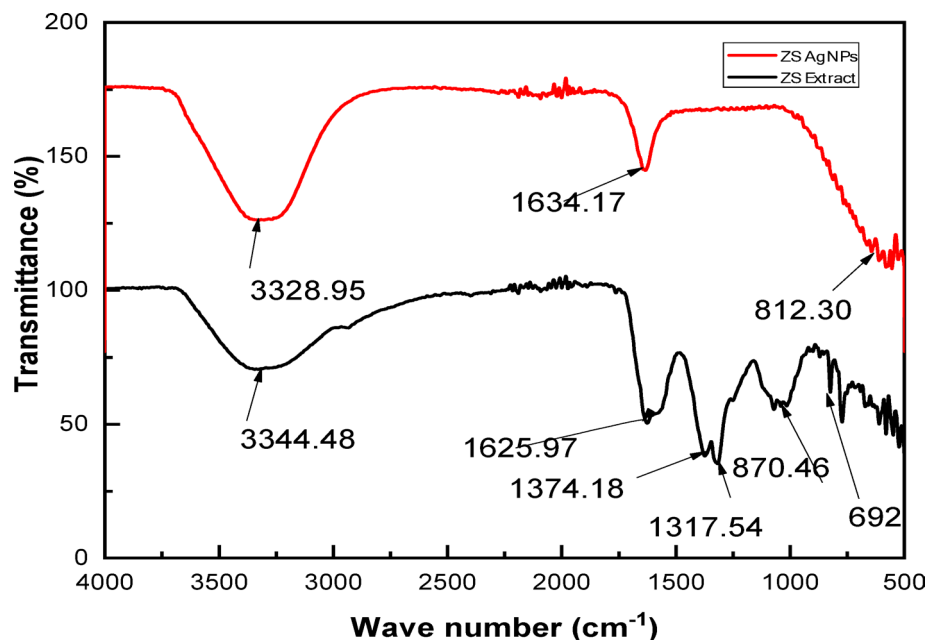


**Fig. 4.** FT-IR analysis of phyto-synthesized AgNPs and stem extract of *Z. pantandra*.

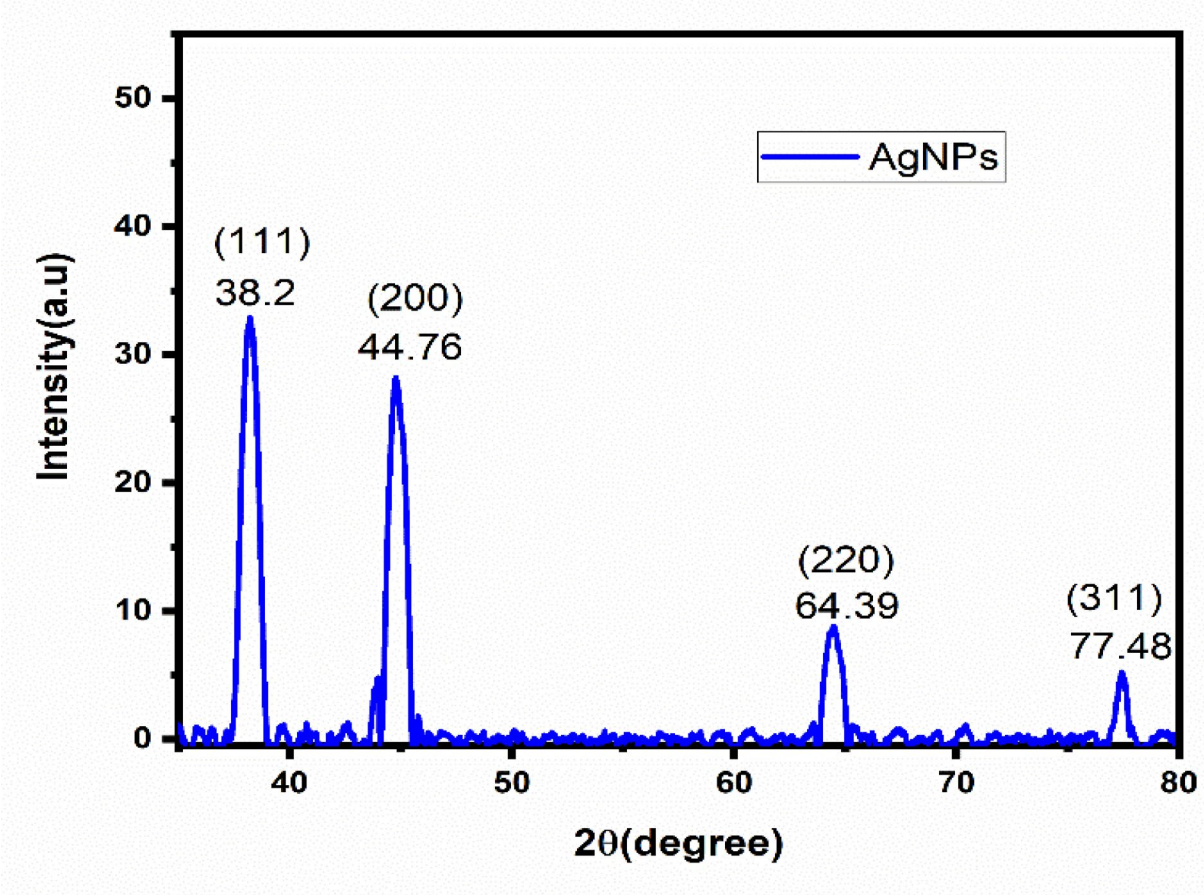


**Fig. 5.** The X-ray diffraction diffractogram of green-synthesized AgNPs using *Z. pantandra* stem extract.

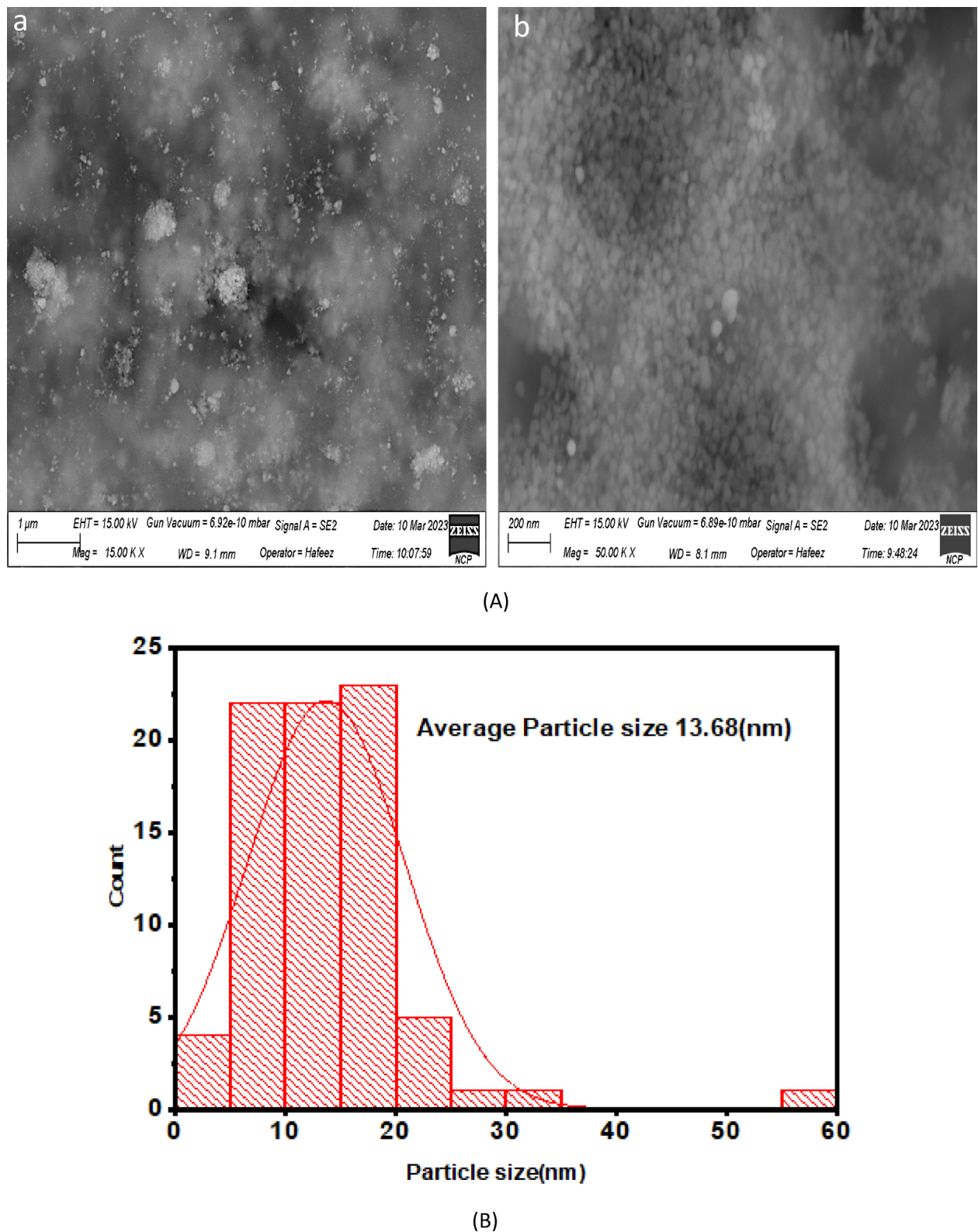


**Fig. 6.** (A) The FESEM image of green-synthesized AgNPs using *Z.pantandra* stem extract (a)  $1\text{ }\mu\text{m}$  (b)  $200\text{ nm}$ . (B) Particle's size distribution of green-synthesized AgNPs using *Z.pantandra* stem extract.

size for *Peganum harmala* derived AgNPs. Salih et al.<sup>47</sup> demonstrated that shape of *Juniperus procera* derived AgNPs was spherical having particle size 19 to 26 nm. This indicated that particle size and morphology depends upon the bioactive compounds present in plant extract<sup>48,49</sup>.

### The EDX analysis

The occurrences of Ag elements were confirmed by the EDX analysis Fig. 7. The Ag peak around binding energy 3kev with an atomic mass percentage of 35.6 showed the presence of a silver element<sup>50,51</sup>. The EDX spectrum confirms silver as the major component but also indicates the presence of oxygen, carbon, potassium, sodium and trace amounts of other elements which were likely due to phytochemical residues from the plant extract acting as capping agents. These results are in agreement with previous studies as EDX spectrum of biosynthesized AgNPs contained other signals of O, Na, Mg, Cu, Al, Cl and Si<sup>52</sup>.

### Mechanism of biosynthesized AgNPs formation

The bioactive compounds found in ZSE as revealed by FT-IR analysis such as alcohol, phenols, and other aromatic compounds donated electrons to silver ions ultimately reducing them to metallic silver. The high basic media (pH 9) ensured binding of the anionic functional groups of ZSE with Ag<sup>+</sup> resulting in the formation of a large number of nuclei for AgNPs. The phytochemicals found in plant extracts function as reducing and stabilizing agents during the green synthesis of silver nanoparticles<sup>53</sup>. This study suggested that biosynthesis of the AgNPs took place in three stages (1) induction phase during which generation of the Ag seeds occurred as a result of the reduction of silver ions due to redox properties of the bioactive compounds found in ZSE (2) growth phase resulting in growing of small Ag seeds into larger aggregates (3) termination phase during which surface stabilization of the Ag aggregates occurred due to capping with bioactive compounds of plant origin, which also play important role in the determination of size and morphology of the nanoparticles<sup>54</sup>.

### Antimicrobial potential of the AgNPs

#### Antibacterial activity

The green-synthesized AgNPs inhibited the growth of tested bacteria Fig. 8. Moreover, the antibacterial potential of green-synthesized AgNPs was more significant than the AgNO<sub>3</sub> solution and *Z. pentandra* stem extract when tested alone. Maximum bacterial growth inhibition was recorded at the highest concentration of the AgNPs, i.e., 1000 µg/mL. The AgNPs at 1000 µg/mL showed 30.9 mm, 27.6 mm, and 25 mm growth-inhibition zones against *S. aureus*, *K. pneumonia*, and *E. coli*. The negative control showed no bacterial growth inhibition. The *Z. pentandra* stem extract showed a 17 mm, 14 mm, and 13 mm zone of growth inhibition against *S. aureus*, *K. pneumonia*, and *E. coli*. The pure AgNO<sub>3</sub> solution showed 19 mm, 17 mm, and 18 mm zones of inhibition against

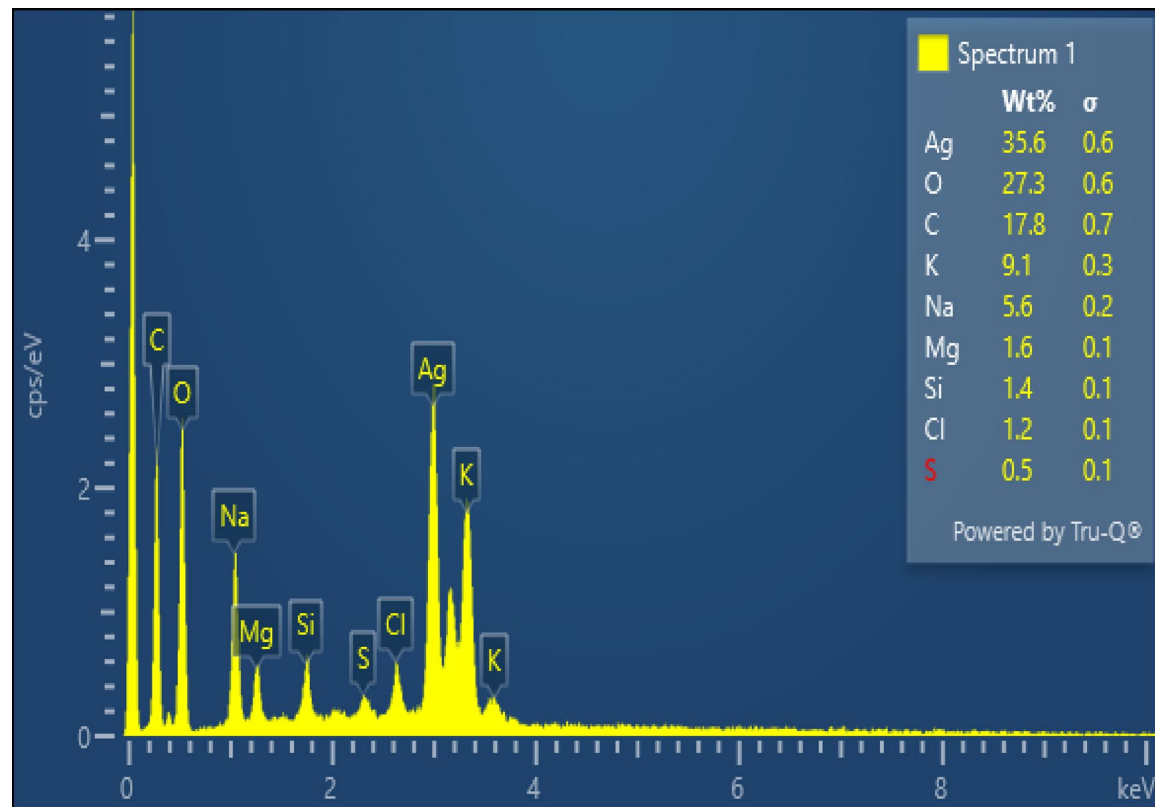


**Fig. 7.** The EDX spectrum of the green-synthesized AgNPs using *Z. pentandra* stem extract.

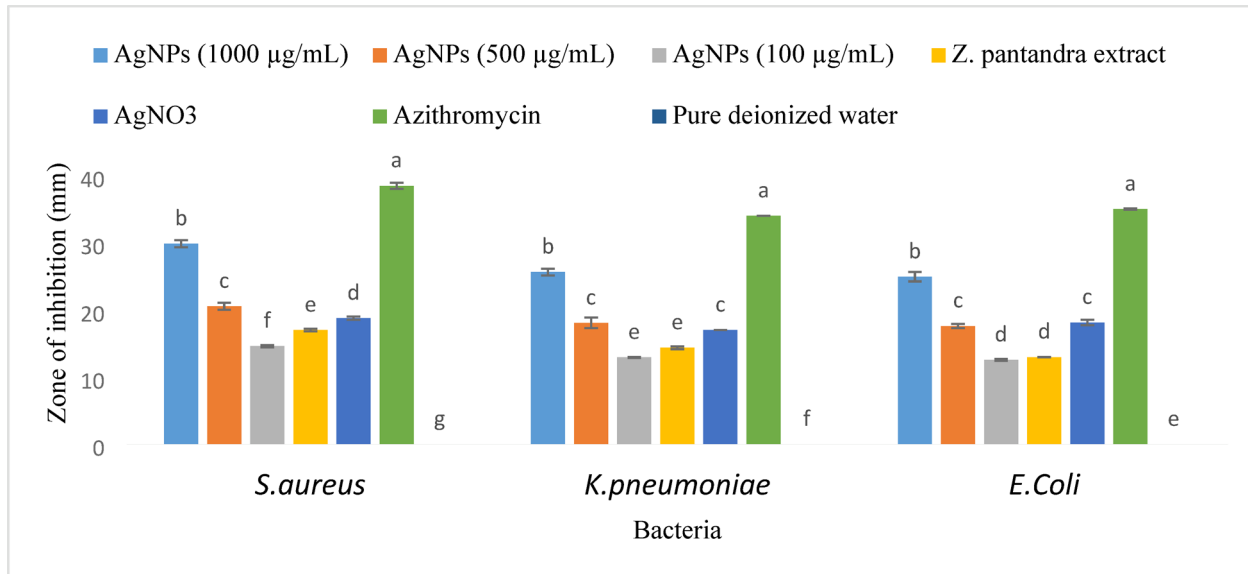


**Fig. 8.** Antibacterial activity of biosynthesized AgNPs,  $\text{AgNO}_3$ , and *Z. pentandra* stem extract.

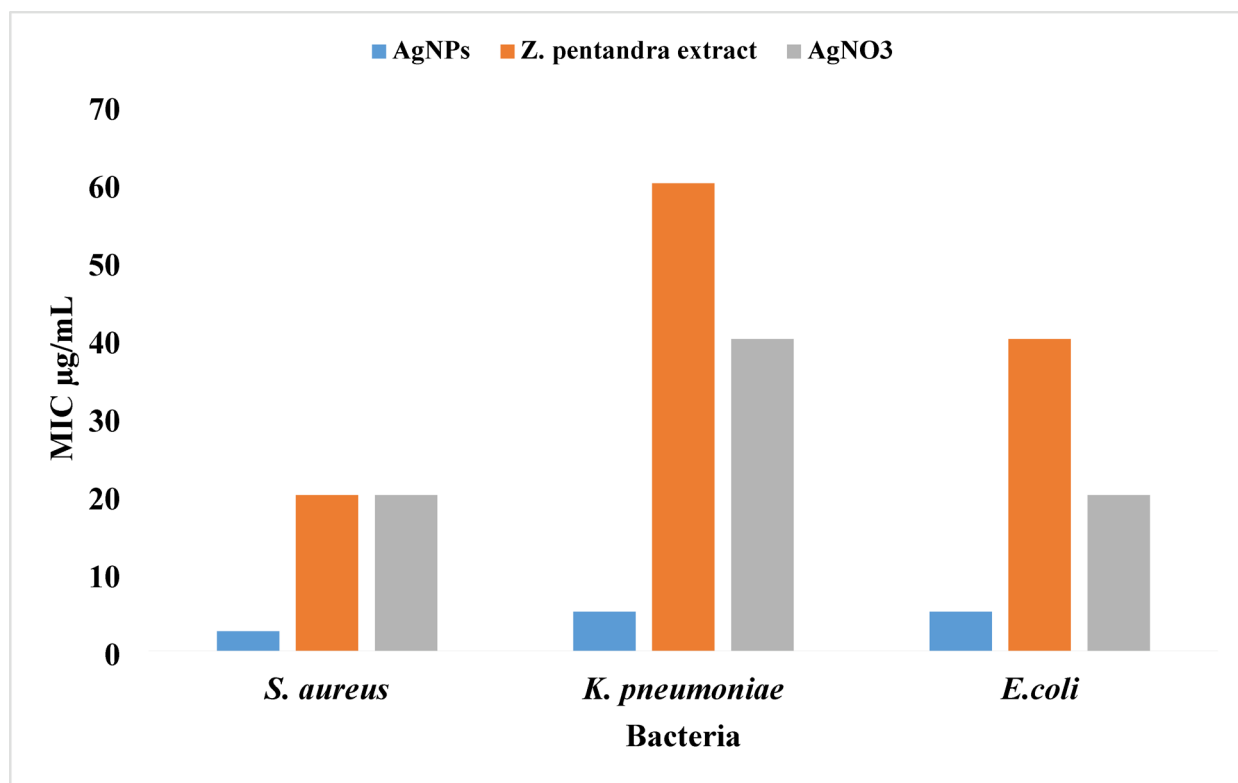


**Fig. 9.** MIC of AgNPs, *Z. pentandra* extract, and  $\text{AgNO}_3$  against the tested bacteria.

*S. aureus*, *K. pneumoniae*, and *E. coli*. This indicated that when used alone, biosynthesized AgNPs were more effective antibacterial agents than the  $\text{AgNO}_3$  and *Z. pentandra* stem extract.

The MIC of green-synthesized AgNPs was  $2.5 \mu\text{g/mL}$  against *S. aureus*, while  $5 \mu\text{g/mL}$  against both *K. pneumoniae* and *E. coli* Fig. 9. The MIC of *Z. pentandra* stem extract was  $20 \mu\text{g/mL}$  against *S. aureus*,  $60 \mu\text{g/mL}$  against *K. pneumoniae*, and  $40 \mu\text{g/mL}$  against *E. coli*. The MIC of  $\text{AgNO}_3$  against the tested bacteria was higher than the green-synthesized AgNPs. The MIC values of ZSE derived AgNPs were lower than those reported by Elsaffany et al.<sup>55</sup> for *S. aureus* ( $31.15 \mu\text{g/mL}$ ), *E. coli* ( $62.5 \mu\text{g/mL}$ ) and *K. pneumoniae* ( $62.5 \mu\text{g/mL}$ ) while testing antibacterial activity of *Bombyx mori* cocoon extract derived AgNPs.

Concentration	% inhibition in linear growth			
	<i>Aspergillus niger</i>	<i>Fusarium solanii</i>	<i>Rhizoctonia solani</i>	<i>Colletotrichum sp.</i>
AgNO <sub>3</sub> (0.001 mM)	32.67 ± 1.76 <sup>d</sup>	24.00 ± 1.73 <sup>f</sup>	28.80 ± 3.47 <sup>e</sup>	37.22 ± 1.19 <sup>e</sup>
<i>Z. pentandra</i> extract (100 mg/100mL)	60.33 ± 0.88 <sup>c</sup>	63.13 ± 1.04 <sup>d</sup>	52.76 ± 16.17 <sup>c</sup>	61.13 ± 1.53 <sup>c</sup>
<i>Z. pentandra</i> extract (50 mg/100mL)	58.00 ± 1.21 <sup>c</sup>	52.66 ± 1.45 <sup>e</sup>	42.20 ± 8.03 <sup>d</sup>	51.76 ± 6.06 <sup>e</sup>
AgNPs (100 mg/100mL)	98.30 ± 2.08 <sup>a</sup>	97.71 ± 2.08 <sup>a</sup>	97.43 ± 13.98 <sup>a</sup>	98.64 ± 9.49 <sup>a</sup>
AgNPs (50 mg/100mL)	81.33 ± 0.93 <sup>b</sup>	85.00 ± 1.45 <sup>c</sup>	83.91 ± 3.47 <sup>b</sup>	84.20 ± 2.85 <sup>b</sup>
Terbinafine (3 mg/mL)	96.00 ± 0.58 <sup>a</sup>	92.69 ± 1.15 <sup>b</sup>	92.43 ± 1.44 <sup>a</sup>	93.80 ± 7.96 <sup>a</sup>

**Table 1.** Antifungal activity of the AgNPs, *Z. pentandra* stem extract and antifungal terbinafine.

Concentration (μg/mL)	DPPH free radicals scavenging (%)		
	AgNPs	<i>Z. pentandra</i> extract	Ascorbic acid
100	62.37 ± 5.23 <sup>c</sup>	43.42 ± 4.21 <sup>c</sup>	70.21 ± 3.24 <sup>c</sup>
200	64.99 ± 2.9 <sup>b</sup>	46.31 ± 3.87 <sup>b</sup>	77.17 ± 4.23 <sup>b</sup>
300	69.19 ± 3.72 <sup>a</sup>	48.38 ± 5.29 <sup>a</sup>	85.25 ± 2.85 <sup>a</sup>
IC50	208.64	218.45	195.04

**Table 2.** The DPPH scavenging activity of *Z. pentandra* stem extract, AgNPs, and ascorbic acid. ± indicates values of standard error.

The green-synthesized AgNPs in this study exhibited small size and uniform distribution making them highly antibacterial. The AgNPs continuously release silver ions that get attached to the negatively charged components of the cell wall causing denaturation of the membrane proteins, a possible mechanism of killing microbes<sup>56,57</sup>. The other possible mechanism may be that AgNPs make bonds with the DNA and other cellular molecules, causing inhibition of cell proliferation<sup>58</sup>. The AgNPs inhibit activity of different enzymes necessary for bacterial metabolism, results in the formation of extensive reactive oxygen species creating oxidative stress that can oxidate cellular components like lipids, proteins and DNA leading to cellular injury<sup>59</sup>. The research findings of the antibacterial activity of phyto-synthesized AgNPs indicated their possible potential biomedical applications.

#### Antifungal activity of AgNPs

The green-synthesized AgNPs and stem extract of *Z. pentandra* were tested for antifungal activity against four fungal species such as *Aspergillus niger*, *Fusarium solanii*, *Rhizoctonia solani*, and *Colletotrichum sp* (Table 1). The antifungal action of the green-synthesized AgNPs was significantly greater ( $p < 0.05$ ) than *Z. pentandra* stem extract and AgNO<sub>3</sub>. The green-synthesized AgNPs at 100 mg/100mL showed 98.30 ± 2.08%, 97.71 ± 2.08, 97.43 ± 13.98 and 98.64 ± 9.49% mycelial growth inhibition of *Aspergillus niger*, *Fusarium solanii*, *Rhizoctonia solani* and *Colletotrichum sp*. The antifungal activity of the green-synthesized AgNPs at 100 mg/100mL was highly comparable to that of the antifungal drug terbinafine. Silver nanoparticles inhibit the cellular growth of fungi by altering the morphology of the cell wall and cell membrane, causing cell lysis<sup>60–62</sup>. The AgNPs bind to the surface proteins, creating pores and interfering with DNA replication. Moreover, AgNPs cause the production of reactive oxygen species, which damage the cell's biomolecules<sup>63,64</sup>. The antifungal potential of the green-synthesized AgNPs suggested their potential application in the control of diseases caused by the tested fungi.

#### Antioxidant activity

Results of DPPH free radicals scavenging activity showed that green-synthesized AgNPs possessed strong antioxidant properties by increasing concentration from 100 to 300 μg/mL. At 300 μg/mL, biosynthesized AgNPs showed a maximum value of DPPH free radical scavenging activity up to 69.19% as compared to *Z. pentandra* stem extract (48.38%). The IC50 values recorded for standard ascorbic acid, AgNPs, and *Z. pentandra* stem extract were 195.04 μg/mL, 208.64 μg/mL, and 218.45 μg/mL. This indicated that the IC50 value of AgNPs was close to the IC50 value of standard ASCA (ascorbic acid) (Table 2). Talib et al.<sup>65</sup> reported IC50 value 264 μg/mL for *Viburnum grandiflorum* derived AgNPs which is higher than the IC50 value reported in present study. This indicated that the antioxidant capability of the AgNPs might be owing to the doping of biomolecules of *Z. pentandra* at their surfaces. Previous researchers have found that photosynthesized silver nanoparticles were highly efficient in free radicals scavenging and alleviation of oxidative stress<sup>66</sup>. This study suggested the potential applications of ZSE-synthesized AgNPs as an alternative to synthetic antioxidants.

#### Antidiabetic activity

The in vitro antidiabetic activity results showed that the α-glucosidase enzyme inhibition activity of both the AgNPs and acarbose remained dose-dependent Fig. 10A. Maximum inhibition in the activity of α-glucosidase was recorded at the 100 μg/mL of the ZSE derived AgNPs and standard drug acarbose. However, the AgNPs showed significantly the highest α-glucosidase inhibition activity over acarbose at all the tested doses. The

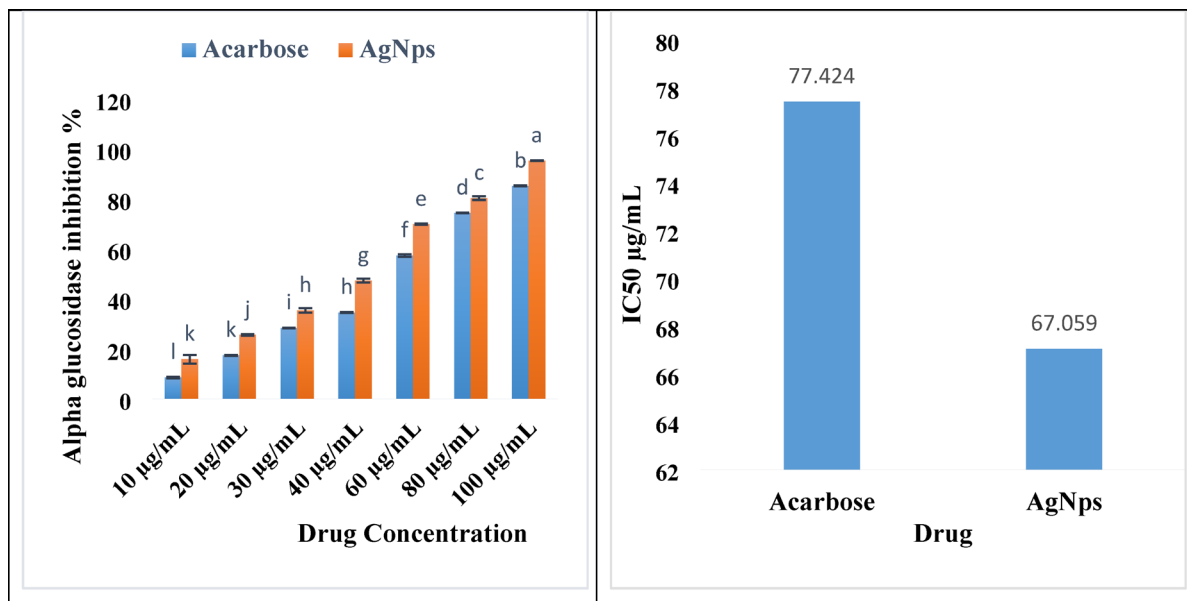


**Fig. 10.** (A)  $\alpha$ -glucosidase inhibition activity of AgNPs and acarbose (B) IC50 values of the AgNPs and acarbose.

IC50 values showed that AgNPs were substantially more effective in inhibiting  $\alpha$ -glucosidase activity than acarbose. The IC50 values calculated for AgNPs and acarbose against glucosidase enzyme were 67.059  $\mu\text{g}/\text{mL}$  and 77.424  $\mu\text{g}/\text{mL}$  Fig. 10B. The AgNPs synthesized by using other plants have also shown  $\alpha$ -glucosidase inhibition activity<sup>67</sup>. Alpha glucosidases are essential enzymes involved in the metabolism of carbohydrates. Therefore, their inhibition is studied as a critical factor for diabetic treatment<sup>68</sup>. Owing to the potentially harmful side effects of the present synthetic antidiabetic medications such as miglitol and acarbose, it is necessary to identify their natural and effective alternatives. Silver nanoparticles generated from medicinal plants are a safe and effective way to treat diabetes<sup>69</sup>. These findings support using ZSE derived AgNPs as a safe and effective antidiabetic treatment for diabetes.

## Conclusion

The present research demonstrated the efficacy of ZSE in the green-synthesis of AgNPs. The green-synthesized AgNPs were characterized by UV-Vis spectroscopy, FT-IR, XRD, FESEM and EDS analysis. The green-synthesized AgNPs were spherical in shape, with mean particle size of 13.68 nm. The FT-IR analysis indicated various biomolecules involved in the reduction and stabilization of AgNPs. The green-synthesized AgNPs revealed potential antimicrobial activity against pathogenic bacteria and fungi recommending them for further application in the biomedical field. The antioxidant activity of the green-synthesized AgNPs was nearly comparable to that of standard drug ascorbic acid which identify their application in food and pharmaceutical industries. The green-synthesized AgNPs considerably inhibited  $\alpha$ -glucosidase activity surpassing standard antidiabetic drug acarbose. This study concluded that green-synthesis of AgNPs using ZSE is an environment friendly, cost effective and easy approach that diminishes the use of toxic materials. However, additional studies are necessary to evaluate their in Vivo cytotoxicity and antidiabetic potential using animal model.

## Data availability

All data generated or analyzed during this study are included in this published article.

Received: 8 July 2025; Accepted: 24 September 2025

Published online: 30 October 2025

## References

1. Erci, F., Cakir-Koc, R. & Isildak, I. Green synthesis of silver nanoparticles using thymbra Spicata L. var. Spicata (zahter) aqueous leaf extract and evaluation of their morphology-dependent antibacterial and cytotoxic activity. *Artif. Cells Nanomed. Biotechnol.* **46** (sup1), 150–158 (2018).
2. Alhalili, Z. Metal oxides nanoparticles: general structural Description, Chemical, Physical, and biological synthesis Methods, role in pesticides and heavy metal removal through wastewater treatment. *Molecules Mar.* **30** (7), 3086. <https://doi.org/10.3390/molecules28073086> (2023).
3. Bratovic, A. Different applications of nanomaterials and their impact on the environment. *Int. J. Mater. Sci. Eng.* **5** (1), 1–7 (2019).
4. Dubey, S. et al. Breaking barriers in Eco-Friendly synthesis of Plant-Mediated Metal/Metal Oxide/Bimetallic nanoparticles: Antibacterial, Anticancer, mechanism Elucidation, and versatile utilizations. *J. Nanomaterials.* **24**, 1–48 (2024).

5. Khodeer, D. M. et al. Characterization, antibacterial, antioxidant, antidiabetic, and anti-inflammatory activities of green synthesized silver nanoparticles using Phragmanthera austroarabica AG mill and JA Nyberg extract. *Front. Microbiol.* **13**, 1078061 (2023).
6. Mahdiani, M., Soofivand, F., Ansari, F. & Salavati-Niasari, M. Grafting of CuFe12O19 nanoparticles on CNT and graphene: eco-friendly synthesis, characterization and photocatalytic activity. *J. Clean. Prod.* **176**, 1185–1197 (2018).
7. Malhotra, S. P. K. & Alghuthaymi, M. A. Biomolecule-assisted biogenic synthesis of metallic nanoparticles. In *Agri-waste and Microbes for Production of Sustainable Nanomaterials* 139–163. (2022).
8. Zhang, X. F., Liu, Z. G., Shen, W. & Gurunathan, S. Silver nanoparticles: synthesis, characterization, properties, applications, and therapeutic approaches. *Int. J. Mol. Sci.* **17** (9), 1534 (2016).
9. Ying, S. et al. Green synthesis of nanoparticles: current developments and limitations. *Environ. Technol. Innov.* **26**, 102336 (2022).
10. Krishnaraj, C. et al. S. B. B. Synthesis of silver nanoparticles using acalypha indica leaf extracts and its antibacterial activity against water borne pathogens. *Colloids Surf. B* **76** (1), 50–56 (2010).
11. Pirtarighat, S., Ghannadnia, M. & Baghshahi, S. Green synthesis of silver nanoparticles using the plant extract of salvia spinosa grown in vitro and their antibacterial activity assessment. *J. Nanostructure Chem.* **9**, 1–9 (2019).
12. Rautela, A. & Rani, J. Green synthesis of silver nanoparticles from tectona grandis seeds extract: characterization and mechanism of antimicrobial action on different microorganisms. *J. Anal. Sci. Technol.* **10** (1), 1–10 (2019).
13. Rónavári, A. et al. Green silver and gold nanoparticles: biological synthesis approaches and potentials for biomedical applications. *Molecules* **26** (4), 844 (2021).
14. Husain, S. A. S. Cyanobacteria as a bioreactor for synthesis of silver nanoparticles—an effect of different reaction conditions on the size of nanoparticles and their dye decolorization ability. *J. Microbiol. Met.* (2020).
15. Gong, P. et al. Preparation and antibacterial activity of Fe3O4@Ag nanoparticles. *Nanotechnology* **18** (28), 285604 (2007).
16. Asif, M. et al. Green synthesis of silver nanoparticles (AgNPs), structural characterization, and their antibacterial potential. *Dose-Response* **20** (2), 15593258221088709 (2022).
17. Bhati, P. et al. Green synthesis of silver NPs using aqueous extract of Artemisia scoparia for hydrogenation of aromatic nitro compounds and their biological activity. *Front. Microbiol.* **16**, 1584066 (2025).
18. Mahmood, A. et al. Ethno medicinal survey of plants from district bhimber Azad Jammu and Kashmir, Pakistan. *J. Med. Plants Res.* **5** (11), 2348–2360 (2011).
19. Seifu, T., Asres, K. & Gebre-Mariam, T. Ethnobotanical and ethnopharmaceutical studies on medicinal plants of Chifra district, Afar region, North Eastern Ethiopia. *Ethiop. Pharm. J.* **24** (1), 41–58 (2004).
20. Hameed, M. et al. Medicinal flora of the Cholistan desert: a review. *Pak J. Bot.* **43** (2), 39–50 (2011).
21. Shahid, A. et al. Phytochemical profiling of the ethanolic extract of Zaleya Pentandra L. Jaffery and its biological activities by in-vitro assays and in-silico molecular Docking. *Appl. Sci.* **13** (1), 584 (2022).
22. Saleem, H. et al. Pharmacological, phytochemical and in-vivo toxicological perspectives of a xero-halophyte medicinal plant: Zaleya Pentandra (L.) Jeffrey. *Food Chem. Toxicol.* **131**, 110535 (2019).
23. Du Preez, B., Dreyer, L. L., Stirton, C. H. & Muasya, A. M. A monograph of the genus Polhillia (Genisteae: Fabaceae). *South. Afr. J. Bot.* **138**, 156–183 (2021).
24. Singh, R. et al. Synthesis of silver nanoparticles using extract of ocimum kilimandscharicum and its antimicrobial activity against plant pathogens. *SN Appl. Sci.* **1**, 1–12 (2019).
25. Azad, A., Zafar, H., Raza, F. & Sulaiman, M. Factors influencing the green synthesis of metallic nanoparticles using plant extracts: a comprehensive review. *Pharm. Front.* **05** (02), (2023).
26. Revati, S., Bipin, C., Chitra, P. B. & Minakshi B. In vitro antibacterial activity of seven Indian species against high level gentamicin resistant strains of enterococci. *Archives Med. Sci.* **11** (4), 863–868 (2015).
27. Washington, J. A. Dilution susceptibility test: agar and macro-broth dilution procedures. *Am. Soc. For. Microbiol.*, (1980).
28. Brand-Williams, W. Use of a free radical method to evaluate antioxidant activity. *Food Sci. Technol.* **28**, 1231–1237 (1999).
29. Manikandan, R., Anand, A. V. & Kumar, S. Phytochemical and in vitro antidiabetic activity of psidium Guava leaves. *Pharmacogn. J.* **8** (4), (2016).
30. Ansar, S. et al. Eco friendly silver nanoparticles synthesis by brassica Oleracea and its antibacterial, anticancer and antioxidant properties. *Sci. Rep.* **10** (1), 18564 (2020).
31. Naika, H. R. et al. Green synthesis of CuO nanoparticles using gloriosa Superba L. extract and their antibacterial activity. *J. Taibah Univ. Sci.* **9** (1), 7–12 (2015).
32. Salari, S., Bahabadi, S. E., Samzadeh-Kermani, A. & Yosefzai, F. In-vitro evaluation of antioxidant and antibacterial potential of greensynthesized silver nanoparticles using prosopis Farcta fruit extract. *Iran. J. Pharm. Res. IJPR.* **18** (1), 430 (2019).
33. Tesfaye, M., Gonfa, Y., Tadesse, G., Temesgen, T. & Periyasamy, S. Green synthesis of silver nanoparticles using Vernonia amygdalina plant extract and its antimicrobial activities. *Heliyon* **9** (6), (2023).
34. Ahmed et al. (2022).
35. Ibrahim, H. M. Green synthesis and characterization of silver nanoparticles using banana Peel extract and their antimicrobial activity against representative microorganisms. *J. Radiation Res. Appl. Sci.* **8** (3), 265–275 (2015).
36. Kumari, R., Brahma, G., Rajak, S., Singh, M. & Kumar, S. Antimicrobial activity of green silver nanoparticles produced using aqueous leaf extract of hydrocotyle rotundifolia. *Orient. Pharm. Experimental Med.* **16**, 195–201 (2016).
37. Vänlalveni, C. et al. Green synthesis of silver nanoparticles using plant extracts and their antimicrobial activities: A review of recent literature. *RSC Adv.* **11** (5), 2804–2837 (2021).
38. Sher, N., Ahmed, M., Mushtaq, N. & Khan, R. A. Cytotoxicity and genotoxicity of green synthesized silver, gold, and silver/gold bimetallic NPs on BHK-21 cells and human blood lymphocytes using MTT and comet assay. *Appl. Organomet. Chem.* **37** (2), e6968 (2023).
39. Dikshit, P. K. et al. Green synthesis of metallic nanoparticles: applications and limitations. *Catalysts* **11** (8), 902 (2021).
40. Nahar, K., Aziz, S., Bashar, M., Haque, M. A. & Al-Reza, S. M. Synthesis and characterization of silver nanoparticles from cinnamomum Tamala leaf extract and its antibacterial potential. *Int. J. Nano Dimension.* **11** (1), 88–98 (2020).
41. Venkatadri, B. et al. Green synthesis of silver nanoparticles using aqueous rhizome extract of Zingiber officinale and curcuma longa, invitro anti-cancer potential on human colon carcinoma HT-29 cells. *Saudi Jurnal Biol. Sci.* **27** (11), 2980–2986 (2020).
42. Hemlata, Meena, P. R., Singh, A. P. & Tejavath, K. K. Biosynthesis of silver nanoparticles using cucumis prophetarum aqueous leaf extract and their antibacterial and antiproliferative activity against cancer cell lines. *ACS Omega.* **5** (10), 5520–5528 (2020).
43. Femi-Adepoju, A. G., Dada, A. O., Otun, K. O., Adepoju, A. O. & Fatoba, O. P. Green synthesis of silver nanoparticles using terrestrial fern (Gleichenia pectinata (Willd.) C. Presl.): characterization and antimicrobial studies. *Heliyon* **5** (4), (2019).
44. Firdous, H. et al. Green synthesis and characterization of Ag nanoparticles using Carissa spinarum L. Leaf extract: evaluation for their antimicrobial and antioxidant activities. *Microsc. Res. Tech.* **88** (8), 2285–2296 (2025).
45. Ahmad, K. et al. Green synthesis and characterization of silver nanoparticles through the Piper Cubeba ethanolic extract and their enzyme inhibitory activities. *Front. Chem.* **11**, 1065986 (2023).
46. Azizi, M., Sedaghat, S., Tahvildari, K., Derakhshi, P. & Ghaemi, A. Synthesis of silver nanoparticles using peganum Harmala extract as a green route. *Green Chem. Lett. Rev.* **10** (4), 420–427 (2017).
47. Salih, A. M. et al. Biogenic silver nanoparticles improve bioactive compounds in medicinal plant Juniperus procera in vitro. *Front. Plant Sci.* **13**, 962112 (2022).

48. Alharbi, N. S., Alsubhi, N. S. & Felimban, A. I. Green synthesis of silver nanoparticles using medicinal plants: characterization and application. *J. Radiation Res. Appl. Sci.* **15** (3), 109–124 (2022).
49. Zarei, Z., Razmjoue, D., Moazeni, M., Azarnivand, H. & Oroojalian, F. *Salvia sclarea* L. (Clary Sage) flower extract-mediated green synthesis of silver nanoparticles and their characterization, antibacterial, antifungal, and scolicidal activities against *Echinococcus granulosus*. *Microbe* **5**, 100216 (2024).
50. Othman, A. M., Elsayed, M. A., Al-Balakoc, N. G., Hassan, M. M. & Elshafei, A. M. Biosynthesis and characterization of silver nanoparticles induced by fungal proteins and its application in different biological activities. *J. Genetic Eng. Biotechnol.* **17**, 1–13 (2019).
51. Riaz, M. et al. Characterizations and analysis of the antioxidant, antimicrobial, and dye reduction ability of green synthesized silver nanoparticles. *Green. Process. Synthesis.* **9** (1), 693–705 (2020).
52. Satpathy, S., Patra, A., Ahirwar, B. & Delwar-Hussain, M. Antioxidant and anticancer activities of green synthesized silver nanoparticles using aqueous extract of tubers of *pueraria tuberosa*. *Artif. Cells Nanomed. Biotechnol.* **46**(sup3), 71–85 (2018).
53. Villagrán, Z. et al. Plant-based extracts as reducing, capping, and stabilizing agents for the green synthesis of inorganic nanoparticles. *Resources* **13** (6), 70 (2024).
54. Khan, M. et al. Green synthesis of silver nanoparticles using *Juniperus procera* extract: their characterization, and biological activity. *Crystals* **12** (3), 420 (2022).
55. Elsaffany, A. H., Abdelaziz, A. E., Zahra, A. A. & Mekky, A. E. Green synthesis of silver nanoparticles using cocoon extract of *Bombyx Mori* L.: therapeutic potential in antibacterial, antioxidant, anti-inflammatory, and anti-tumor applications. *BMC Biotechnol.* **25** (1), 38 (2025).
56. Bapat, R. A. et al. P. An overview of application of silver nanoparticles for biomaterials in dentistry. *Mater. Sci. Eng. C*, **91**, 881–898 (2018).
57. Ghasemi, S. et al. Yousef-beyk, F. Process optimization for green synthesis of silver nanoparticles using *rubus discolor* leaves extract and its biological activities against multi-drug resistant bacteria and cancer cells. *Sci. Rep.* **14** (1), 4130 (2024).
58. Panda, M. K., Dhal, N. K., Kumar, M., Mishra, P. M. & Behera, R. K. Green synthesis of silver nanoparticles and its potential effect on phytopathogens. *Mater. Today Proceeding* **35**, 233–238 (2021).
59. Alhwibi, M. S. et al. Green biosynthesis of silver nanoparticle using *commiphora myrrh* extract and evaluation of their antimicrobial activity and colon cancer cells viability. *J. King Saud University-Science* **32** (8), 3372–3379 (2020).
60. Khan, S. T. & Al-Khedairy, A. A. Metals and metal oxides: important nanomaterials with antimicrobial activity. In *Antimicrobial Nanoarchitectonics*. 195–222 (2017).
61. Bonilla, J. J. A. et al. O. Green synthesis of silver nanoparticles using maltose and cysteine and their effect on cell wall envelope shapes and microbial growth of *Candida* spp. *J. Nanosci. Nanotechnol.* **17** (3), 1729–1739 (2017).
62. Hassan, S. A., Hanif, E., Khan, U. H. & Tanoli, A. K. Antifungal activity of silver nanoparticles from *Aspergillus Niger*. *Pak J. Pharm. Sci.* **32** (3), 1163–1166 (2019).
63. Durán, N., Nakazato, G. & Seabra, A. B. Antimicrobial activity of biogenic silver nanoparticles, and silver chloride nanoparticles: an overview and comments. *Appl. Microbiol. Biotechnol.* **100**, 6555–6570 (2016).
64. Elamawi, R. M., Al-Harbi, R. E. & Hendi, A. A. Biosynthesis and characterization of silver nanoparticles using *trichoderma longibrachiatum* and their effect on phytopathogenic fungi. *Egypt. J. Biol. Pest Control* **28** (1), 1–11 (2018).
65. Talib, H. et al. Antibacterial, antioxidant, and anticancer potential of green fabricated silver nanoparticles made from *viburnum grandiflorum* leaf extract. *Bot. Stud.* **65** (1), 4 (2024).
66. Yousaf, H., Mehmood, A., Ahmad, K. S. & Raffi, M. Green synthesis of silver nanoparticles and their applications as an alternative antibacterial and antioxidant agents. *Mater. Sci. Engineering: C*, **112**, 110901 (2020).
67. Thirumal, S. & Sivakumar, T. Synthesis of silver nanoparticles using *Cassia auriculata* leaves extracts and their potential antidiabetic activity. *Int. J. Bot. Stud.* **6** (3), 35–38 (2021).
68. Jini, D., Sharmila, S., Anitha, A., Pandian, M. & Rajapaksha, R. M. H. In vitro and in Silico studies of silver nanoparticles (AgNPs) from *allium sativum* against diabetes. *Sci. Rep.* **12** (1), 22109 (2022).
69. Essghaier, B., Hannachi, H., Nouir, R., Mottola, F. & Rocco, L. Green synthesis and characterization of novel silver nanoparticles using *Achillea Maritima* subsp. *Maritima* aqueous extract: antioxidant and antidiabetic potential and effect on virulence mechanisms of bacterial and fungal pathogens. *Nanomaterials* **13** (13), 1964 (2023).

## Acknowledgements

The authors express their gratitude to the Princess Nourah bint Abdulrahman University Researchers Supporting Project number (PNURSP2025R101), Princess Nourah bint Abdulrahman University, Riyadh, Saudi Arabia.

## Author contributions

Conceptualization, Faizan Ullah; Data curation, Shah Saud, Neelam Neelam; Formal analysis, Modhi O. Alotaibi, Nashad Ali; Investigation, Neelam Neelam, Faizan Ullah; Methodology, Shah Saud, Sultan Mehmood; Tahir Iqbal, Mudassir Aslam, Sultan Mehmood, Umar Nawaz Khan; Project administration, Taufiq Nawaz; Adel M. Ghoneim, Esawy Mahmoud; Resources; Supervision, Faizan Ullah; Validation, Taufiq Nawaz; Shah Saud; Writing – original draft Neelam Neelam, Faizan Ullah; Writing – review & editing, Shah Fahad; Adel M. Ghoneim, Esawy Mahmoud; Modhi O. Alotaibi.

## Funding

This research has been supported by the Princess Nourah bint Abdulrahman University Researchers Supporting Project number (PNURSP2025R101), Princess Nourah bint Abdulrahman University, Riyadh, Saudi Arabia.

## Declarations

### Competing interests

The authors declare no competing interests.

### Permissions or licenses

The experiment was started, after taking permission from University of Science and Technology Bannu, Khyber Pakhtunkhwa, Pakistan.

### Identification of the plant material

Before collection, the plant was identified by Dr. Tahir Iqbal (Taxonomist), using the standard protocol at the Department of botany, University of Science and Technology Bannu, Pakistan.

### Additional information

Correspondence and requests for materials should be addressed to F.U. or S.F.

Reprints and permissions information is available at [www.nature.com/reprints](http://www.nature.com/reprints).

**Publisher's note** Springer Nature remains neutral with regard to jurisdictional claims in published maps and institutional affiliations.

**Open Access** This article is licensed under a Creative Commons Attribution-NonCommercial-NoDerivatives 4.0 International License, which permits any non-commercial use, sharing, distribution and reproduction in any medium or format, as long as you give appropriate credit to the original author(s) and the source, provide a link to the Creative Commons licence, and indicate if you modified the licensed material. You do not have permission under this licence to share adapted material derived from this article or parts of it. The images or other third party material in this article are included in the article's Creative Commons licence, unless indicated otherwise in a credit line to the material. If material is not included in the article's Creative Commons licence and your intended use is not permitted by statutory regulation or exceeds the permitted use, you will need to obtain permission directly from the copyright holder. To view a copy of this licence, visit <http://creativecommons.org/licenses/by-nc-nd/4.0/>.

© The Author(s) 2025